

# An Application of Neural and Probabilistic Unsupervised Methods to Environmental Factor Analysis of Multi-spectral Images

Luca Pugliese<sup>1</sup>, Silvia Scarpetta<sup>3</sup>, Anna Esposito<sup>1,2</sup>, and Maria Marinaro<sup>1,3</sup>

<sup>1</sup> IIASS, Istituto Internazionale per gli Alti Studi Scientifici "E.R.Caianello", Via G.Pellegrino, 19 – Vietri sul Mare - Salerno

{iiass.luca@tiscali.it, iiass.annaesp@tin.it

<sup>2</sup> Dipartimento di Psicologia, Seconda Università di Napoli, Via Vivaldi 43, Caserta

<sup>3</sup> Dipartimento di Fisica "E.R.Caianello", Università degli Studi di Salerno, Via S.Allende, Salerno, Italy and INFN and INFN Sezione di Salerno, Italy  
silvia@sa.infn.it, marinaro@sa.infn.it

**Abstract.** In this paper we test the performance of two unsupervised clustering strategies for the analysis of LANDSAT multispectral images of the Temples of Paestum Area in Italy. The classification goal is to identify environmental factors (soils, vegetation types, water) on the images, exploiting the features of the seven LANDSAT spectral bands. The first strategy is a fast migrating means technique based on a Maximum Likelihood Principle (ISOCLUST algorithm), and the second is the Kohonen Self Organizing Map (SOM) neural network. The advantage of using the SOM algorithm is that both the information on classes and the similarity between the classes are obtained (since proximity corresponds to similarity among neurons). By exploiting the information on class similarity it was possible to automatically colour each cluster identified by the net (assigning a specific colour to each of them) thus facilitating a successive photo-interpretation.

## 1 Introduction

The analysis of remotely sensed multispectral data is of great interest for improving the knowledge of the Earth surface and remarkably contributes to the development of policies for planning and monitoring environmental resources [12]. The standard approach to the analysis of such images involves the grouping of image data into a finite number of discrete clusters or classes that identify the distribution, over the land, of environmental factors such as soils, vegetation, urban areas, and rivers. For several decades, such clustering has been implemented using classical statistical approaches, mostly based on the Maximum Likelihood Principle (MLP) [1-2], assuming that clusters can be modelled as a multivariate normal distribution. However, geographical phenomena are not randomly distributed in nature and are not always displayed in the image with a normal distribution. Therefore, other methods have been suggested to overcome their limitations, among which Artificial Neural Networks (ANN). Recent developments in the field have shown that supervised NN algorithms

are able to perform a better classification than statistical approaches due to the fact that no assumption is made on the cluster distribution in the image data [3-5]. However supervised classification with neural networks requires labelled data that generally are not available and therefore several authors have proposed methodologies based on unsupervised techniques and demonstrated their effectiveness in multispectral satellite images classification to land-cover categories [6], [7]. At the light of these last reported studies and with the aim to study the possibility to use remotely sensed data for the mapping of archaeological features we investigate the performance of two unsupervised techniques for land-cover classification in the *Piana del Sele* (Paestum), Italy. The present paper is organized as follow: Section 2 describes the area of interest and the image data available; Section 3 and Section 4 briefly report on the two selected unsupervised strategies and on the results obtained; and finally Section 5 reports our considerations and evaluation on the two proposed strategies.

## 2 Data Source and Study Area

A LANDSAT 7 Enhanced Thematic Mapper (ETM+) image from January 2003 was analyzed for this study using IDRISI Kilimanjaro geo-analytic and image processing system (<http://www.clarklabs.org>). The scene covers the south part of Campania region (Italy), specifically the area named *Piana del Sele* identified in the UTM (Universal Transverse Mercator) reference system, zone 33 North, with the following coordinates: Upper Left Corner(m): (498728.6411429; 4468395.1036465); Lower Right Corner(m): (507790.7439107; 4478689.1775624).

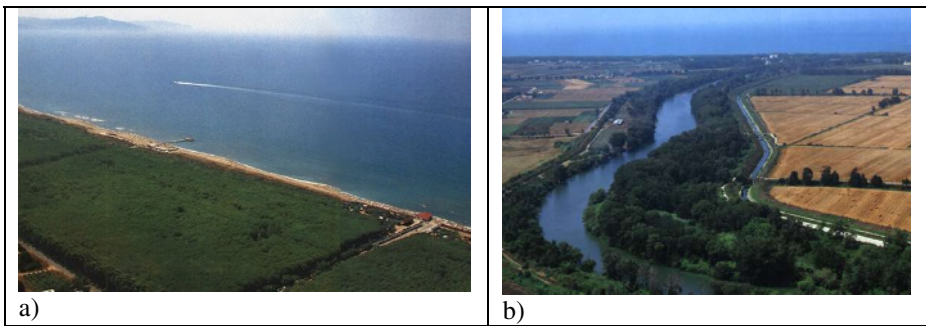


**Fig. 1.** a) Coastal zone of Paestum; b) Sele river (SA, Italy)

This area is primarily an agricultural land (no mountains are situated in the area) with major crops including corn, soybeans, grain, tobacco and canning vegetables, extensively irrigated by the water of the main river of the area, the River Sele. The coastal zone is mostly occupied by pine wood. On the area is also situated an ancient Greek archaeological site that preserves ruins dated 600 BC. During the last 60 years, an urbanization phenomenon has arisen in the area, producing a sparse dissemination of urban fabric and other human artefacts, especially for farming practice (greenhouses). Two aerial photos of zone are shown in Figure 1. The site contains many types of land

cover, among which water, urban areas, irrigated vegetation, unproductive terrain, agricultural areas with both permanent and seasonal crops, natural grassland, and conifers. The urban area is made up of discontinuous fabric mixed with vegetation. Besides, agricultural lands, natural grassland, and artificial surfaces are highly mixed, making difficult the land cover classification in some cases, especially in consideration of the ground resolution reported below.

LANDSAT 7 carries the Enhanced Thematic Mapper Plus instrument – a nadir-viewing multispectral scanning radiometer, providing image data of the Earth’s surface via eight spectral bands (TM1, TM2, TM3, TM4, TM5, TM6, TM7, TM8). The bands are for the visible (TM1, TM2, TM3), the near infrared (TM4), the mid infrared (TM5, TM7), and the thermal infrared (TM6) regions of the electromagnetic spectrum, as well the panchromatic region (TM8). Table 1 lists the ETM+ bands, spectral ranges, and nominal ground resolution.

**Table 1.** LANDSAT 7 ETM+ bands, spectral ranges, and ground resolution (from Eurmoimage©)

Band Number	Spectral Range ( $\mu\text{m}$ )	Ground Resolution (m)
TM1 (Blue -Visible)	0.450 – 0.515	30
TM2 (Green - Visible)	0.525 – 0.605	30
TM3 (Red - Visible)	0.630 – 0.690	30
TM4 (Near Infrared)	0.760 – 0.900	30
TM5 (Mid Infrared)	1.550 – 1.750	30
TM6 (Thermal Infrared)	10.42 – 12.50	60
TM7 (Mid Infrared)	2.080 – 2.350	30
TM8 (Panchromatic )	0.520 – 0.900	15

Data are quantized at 8 bits. The size of an image, for each band, is 286 lines x 105820 pixels. We used seven of these bands as input to the two unsupervised techniques to be able to include all the spectral ranges in the analysis.

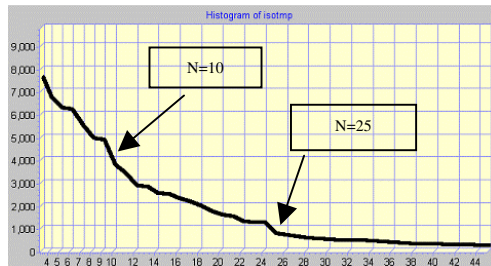


**Fig. 2.** One-dimensional histogram produced by the first step of the ISOCLUST module. The x-axis reports the number of the clusters identified by the histogram peak procedure and the y-axis reports the number of pixels in each cluster.

Therefore only the panchromatic band (TM8) was excluded, since it covers the same spectral range of TM2, TM3 and TM4. The seven images used as input data were acquired by EUROIMAGE© (<http://www.eurimage.com/>) and geometrically corrected at level 1G using a Nearest Neighbour re-sampling algorithm [8]. A COST [9] atmospheric correction was performed by the authors on the bands TM1 and TM2 due to the presence of haze. No processing was performed on the images.

### 3 ISOCLUST Algorithm Description and Results

ISOCLUST stands for Iterative Self Organizing CLUSTERing and is a module proposed in the IDRISI Kilimanjaro image processing system implementing an algorithm that performs unsupervised classification. The algorithm is essentially based on an iterative optimization clustering procedure. Its originality lies in the definition of the initial condition (seeding step) from which the iterative process goes on to the final classification.

Normally, the seeding step is a random or systematic segmentation of the image to be classified, whilst the ISOCLUST module performs a true one-shot clustering process based on a histogram peak technique proposed by Richards [8]. For each input file, the procedure computes the histogram according to a specified number of gray levels. These histograms are then merged together creating a multidimensional histogram where pixels are accumulated. Peaks are then identified on this multidimensional histogram as those locations with a frequency higher than that of all the non-diagonal neighbors except one. Each peak with its neighborhood identifies a cluster and a one-dimensional histogram is plotted where the clusters identified by the histogram peak procedure, are ordered according to the number of pixels accumulated in each of them. Figure 2 shows the clusters identified in our experiment. The x-axis reports the number of the clusters identified by the histogram peak procedure and the y-axis reports the number of pixels in each cluster. In order to fix the number  $N$  of clusters needed for our classification significant breaks are identified in the curve in Figure 2, presumably representing major changes in the level of details for the description of the scene. For example, in our case, we identified in Figure 2 two major breaks at  $N=10$  and at  $N=25$  clusters. These values specify the number of clusters to be retained for the subsequent refining iterations of the ISOCLUST procedure. For each cluster identified in the first seeding step, a set of spectral signatures with their variance/covariance matrices are calculated and the pixels are regrouped in  $N$  new clusters modeled according to the Maximum Likelihood Principle. Due to the efficiency of the seeding step, very few iterations are required to produce a stable result. In our case only three iterations were performed. The ISOCLUST results for  $N=25$  and  $N=10$  clusters are displayed in Figure 3.

The photo interpreter can easily recognize in Figure 3a) the coast and the sea is described by four different clusters (or colours) that are likely to represent differences in water turbidity, sea level and temperature (an information contained in the TM6 band, see Table 1). Starting from the coastline and proceeding inward, it is possible to identify the cluster describing the sea shore (red pink) that also contains the big regular structure visible in the upper right of Figure 3a, other similar smaller structures, and urban areas. The cluster groups together sea shore, and greenhouses and buildings

(artificial surfaces). Two clusters (indigo and bright blue) are descriptive of the pine wood and the River is identified in yellow (the upper left part of Figure 3a). However, all the other characteristics of the land are confused and difficult to be detected without the help of ancillary data.

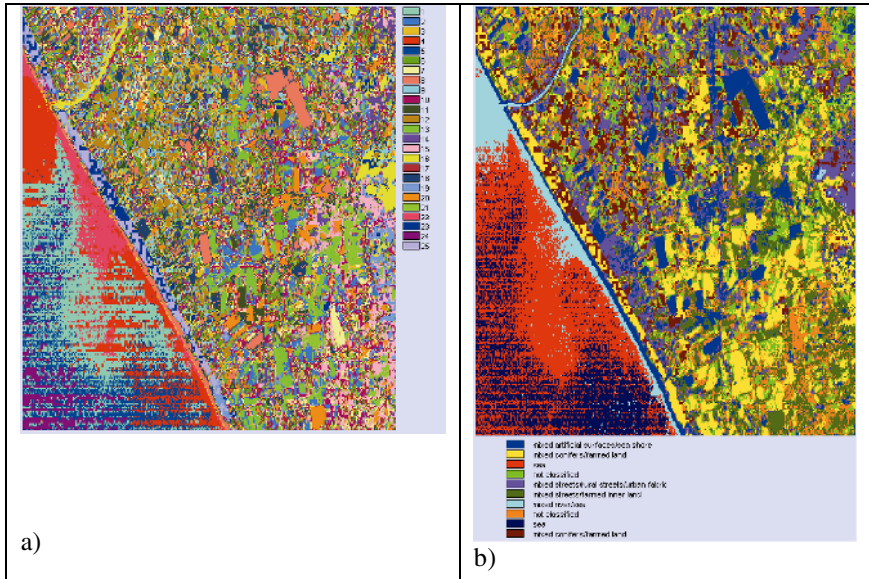


**Fig. 3.** Results obtained with Idrisi ISOCLUST algorithm using 25 spectral classes

To be able to coarsely detect the main characteristics of the land, a second experiment involving only  $N=10$  clusters was performed. Results are displayed in Figure 3b showing that a reduced number of clusters worsens the quality of the clusterization. As it could be noticed in the legend, except for the sea, all the other classes are mixed or unrecognizable.

#### 4 SOM Algorithm Description and Results

The Self-Organizing Map (SOM) [10] is an unsupervised neural network algorithm that has turned out to be an efficient tool, in various applications, for data exploration tasks. It carries out a nonlinear mapping of input data onto a two-dimensional grid. The mapping preserves the most important topological and metric relationships of the data. The SOM map consists of a regular grid of processing units known as *neurons* or *nodes*. A prototype vector is associated with each neuron and the map attempts to represent the data structure with optimal accuracy using a restricted set of neurons. At the same time the neurons are ordered on the grid so that similar prototypes are associated to the neighbouring neurons and dissimilar prototypes to neurons far from each other. The SOM learning algorithm achieves two important steps: (a) it clusters the input data into neurons and (b) spatial order, in the sense that similar input patterns

tend to produce response in neighbouring neurons. In this paper, the SOM is used to visualize the intrinsic structure of the multispectral data of the satellite image, and get an unsupervised classification of the corresponding pixels.

To be able to compare the ISOCLUST with the SOM results we set the SOM architecture to  $N=24$  and  $N=10$  neurons respectively, assuming that each neuron represent a cluster. The net inputs were the 7 bands described above. The SOM algorithm organizes the resulting maps as a  $4 \times 6$  and a  $2 \times 5$  bidimensional exagonal tasseled grids respectively. The resulting maps with  $N=24$  and  $N=10$  neurons are shown in Figure 4a and 4d respectively. Green hexagons represent the neurons and their size the number of pixels accumulated in each of them.

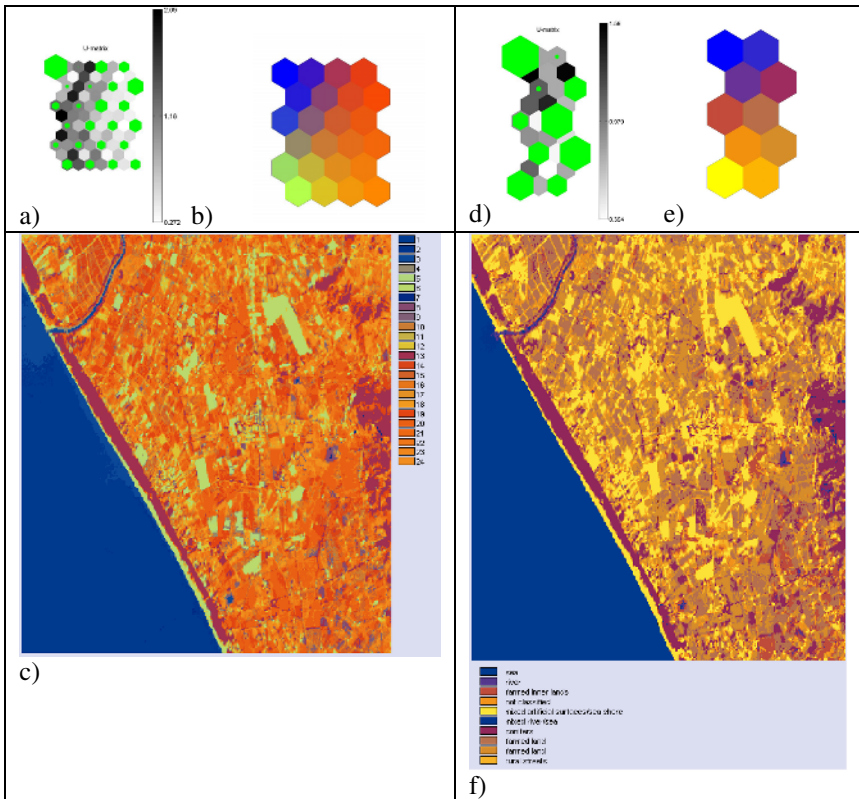


**Fig. 4.** a) A SOM map with 24 neurons, the green hexagons are the neurons. b) Map resulting from the Colouring Procedure described in the text. c) Original scene coloured according to the SOM colour map in panel b). Panels a), b) and c) are repeated in panels d), e), and f) for 10 neurons.

The different grey levels of the remaining hexagons exemplify the distance between each pair of neurons (i.e. the Euclidean distance between two prototypes), where greater distances correspond to darker hexagons.

Exploiting the SOM similarity propriety [10] a Colouring Procedure based on the Sammon's Projection [13] of the prototypes in a coloured plane was performed. The obtained projection allows to assign similar colours to similar neuron-prototypes on the SOM map. Each neuron was coloured according to the resulting projection of the prototype in the coloured map moving from blue to red for the left upper and the right lower corner respectively. The results are displayed in Figure 4b, and 4e for  $N=24$  and  $N=10$  neurons. The effects of the colouring procedures on the original scene are shown in Figure 4c and 4f for  $N=24$  and  $N=10$  neurons, respectively. The colouring process seems to cluster the maps into a reduced number of classes assigning similar colours to similar classes.

The colouring makes the human interpretation of the land cover easier. Comparing the results in Figure 4c with the prior knowledge of the scene we can see that the water (either of the sea or the river) appears in three different blue tones. Indeed these pixels fall in the three neurons in the upper left part of the map (panel 3b). Agricultural lands all over the image appear with different brown tones and the corresponding pixels fall in close neurons on the SOM map (panel 3b).

The yellow groups together the sea shore, the greenhouses and the urban area, while the magenta groups together the pine wood near the seashore and the mountain wood. In Figure 4c it is also possible to identify the rural streets, as for example at the border of the fields close to the river and two straight lines corresponding to the railway and to a major highway crossing the area. A less detailed but clearer clusterization comes from colouring the original scene with the SOM colour map obtained using 10 neurons as described in Figure 4d, 4e, and 4f.

It can be seen that the principal characteristics of the land cover, detectable in the 24 neurons' classification has been preserved in the 10 neurons' classification, and the clusters merged are those coloured with similar colour tones in the 24 classes case. This merge resulted useful for the interpretation of the original scene since similar structures were grouped together in the same cluster. The small number of clusters allows labeling them in a more precise way. For example, different types of conifers (i.e. seaside pinewood, conifers near some streets, and mountain woods) were all grouped in the same cluster. Three different kinds of farmed lands were attributed to three different clusters. Artificial surfaces (greenhouses and buildings) and seashore are displayed in only one single cluster. The river and the sea give rise to two different clusters. Even though some mixed classes are still present, the pure ones are more numerous than in the corresponding ISOCLUST experiment.

## 5 Conclusions

As shown above, the SOM based approach produces a result that makes the human interpretation of land covers through LANDSAT image easier, since it exploits the topological properties of the data in colouring the classes. In such a way, the interpreter, as in the classical interpretation of colour composite images, can achieve a colour driven labelling of unknown areas with a certain confidence. This property doesn't apply to the ISOCLUST results (see Figure 3 above), leaving to the interpreter the job of assigning the proper significance to each cluster.

In conclusion, both classifiers, even though based on an unsupervised algorithm, have proven to make a good job on the image under study, by revealing many intricate details of the landscape.

## Acknowledgements

This work was partially funded by Centro Regionale di Competenza per l'Innovazione Applicata ai Beni Culturali ed Ambientali. The authors are thankful to the Professor Angela Pontrandolfo, dean of the department of Beni Culturali (Salerno University) and the dott. Alfonso Santoriello for the valuable information on the Paestum area.

## References

1. Fu, K.S., Landgrebe, D.A., Phillips, T.L.: Information Processing of Remotely Sensed Agricultural Data. Proceeding of IEEE, Vol. 57 (1969) 639-653
2. Goldberg, M., Shlien, S.: A Clustering Scheme for Multispectral Images. IEEE Trans. SMC, Vol. 8 (1978) 86-92
3. Benediktsson, J., Philip, H. S., And Okan K. E.: Neural Network Approaches Versus Statistical Methods in Classification of Multi-source Remote Sensing Data. IEEE Transactions on Geoscience and Remote Sensing, Vol. 28:4 (1990) 540-551
4. McClelland, G.E., Dewitt, R.N., Hemmer, T.H., Matheson, L.N. Moe, G.O.: Multispectral Image-Processing with Three-Layer Back-Propagation Network. Proceedings of the International Joint Conference on Neural Networks, New York: I.E.E.E., Vol. 1 (1989) 151-153
5. Kamata, S., Kawaguchi, E.: A Neural Classifier for Multi-Temporal Landsat Images Using Spatial and Spectral Information. Proceedings of International Joint Conference on Neural Networks, Nagoya, Japan (1993) 2199-2202
6. Wang, Y., Jamshidi, M., Neville, P., Bales, C., Morain, S.: Multispectral Landsat Image Classification Using a Data Clustering Algorithm. Proceedings of 3th International Conference on Machine Learning and Cybernetics, Shanghai (2004) 4380-4384
7. Vassilas, N., Charou, E.: A New Methodology for Efficient Classification of Multispectral Satellite Images Using Neural Networks Techniques. Neural Processing Letters, Vol. 9 (1999) 35-43
8. Richards, J.A., Jia X.: Remote Sensing Digital Image Analysis. Springer-Verlag (1999) 58-59, 225,235-236
9. Chavez, P.S. Jr.: Image-Based Atmospheric Corrections Revisited and Revised. Photogrammetric Engineering and Remote Sensing Vol.62(9) (1996) 1025-1036
10. Kohonen, T.: Self-Organizing Maps. Series in Information Sciences, Vol. 30, Springer Verlag, Second Ed. (1997)
11. Mather, P. M.: Computer Processing of Remotely Sensed Images an Introduction. Second Ed., John Wiley Press (1999)
12. Büttner, G., et al: The European Corine Land Cover Project. XXth Congress of International Society for Photogrammetry and Remote Sensing, Istanbul , Turkey (2004)
13. Borg, I., and P. Groenen, P. Modern Multidimensional Scaling. Springer-Verlag, New York (1997).